J. Biochem. 121, 317-324 (1997)

Pore Size of Porous Hydroxyapatite as the Cell-Substratum Controls BMP-Induced Osteogenesis[1]

Eichi Tsuruga,* Hiroko Takita,* Hideaki Itoh,† Yuichi Wakisaka,† and Yoshinori Kuboki*,[2]

*Department of Biochemistry, School of Dentistry, Hokkaido University, Kita 13, Nishi 7, Kita-ku, Sapporo 060; and †Muroran Research Laboratory, The Japan Steel Works, Ltd., 4 Chatsu-machi, Muroran 051

Received for publication, September 30, 1996

To elucidate the biochemical mechanism of osteogenesis, the effect of matrix geometry upon the osteogenesis induced by bone morphogenetic protein (BMP) was studied. A series of five porous hydroxyapatites with different pore sizes, 106-212, 212-300, 300-400, 400-500, and 500-600 μm, was prepared. A block (approximately 5×5×1 mm, 40.0 mg) of each hydroxyapatite ceramics was combined with 4 μg of recombinant human BMP-2 and implanted subcutaneously into the back skin of rat. Osteoinductive ability of each implant was estimated by quantifying osteocalcin content and alkaline phosphatase activity in the implant up to 4 wk after implantation. In the ceramics of 106-212 μm, the highest alkaline phosphatase activity was found 2 wk after implantation, and the highest osteocalcin content 4 wk after implantation, consistent with the results observed with particulate porous hydroxyapatite [Kuboki, Y. *et al.* (1995) *Connect. Tissue Res.* 32: 219-226]. Comparison of the alkaline phosphatase activities at 2 wk and the osteocalcin contents at 4 wk after implantation revealed that the highest amount of bone was produced in the ceramics implants with pore size of 300-400 μm. In the ceramics with smaller or larger pore sizes, the amount of bone formation decreased as the pore size deviated from 300-400 μm. The results indicated that the optimal pore size for attachment, differentiation and growth of osteoblasts and vascularization is approximately 300-400 μm. This study using chemically identical but geometrically different cell substrata is the first demonstration that a matrix with a certain geometrical size is most favorable for cell differentiation.

Key words: bone morphogenetic protein, extracellular matrix, osteogenesis, pore size, porous hydroxyapatite.

To understand the biochemical mechanism of bone formation, it was proposed that, at least, four factors must be taken into consideration (*1*). They are: (i) cells directly involved in bone formation, (ii) matrices produced by the cells, (iii) body fluid that contains mineral ions, and (iv) regulators of general cellular activities as well as the calcification process. These four factors should be analyzed individually, then the interactions between them elucidated (*2-4*), and finally they should be integrated into a whole picture of bone formation. The principle can be applied not only to understanding the mechanism of bone formation but also to reconstructing bone tissue locally *in vivo* and *in vitro*.

To verify the above proposition, we chose ectopic osteo- and chondrogenesis induced by BMP (*5-7*) as our experimental system. This system offers the merits that cells and body fluid are already available in the system, and the only items we must add are the matrix and regulators to induce cartilage and bone formation. Another merit is that the process of bone formation can be observed from the very onset and in a very restricted area.

BMP-induced chondro- and osteogenesis in ectopic tissues such as skin and muscles were originally discovered by Urist *et al.* in 1965 (*8*). The proteins called BMP were found to be members of the TGF-β supergene-family by cloning and sequencing of their DNA (*9*). It was also found that BMP consisted of multiple members of the BMP family, BMP-2 to BMP-13 (*10*). Most of them are active in terms of inducing ectopic osteogenesis. Above all, recombinant BMP-2, -4, and -7 are now available and known to induce ectopic bone formation (*11-13*).

One of the most interesting aspects of BMP-induced chondro- and osteogenesis is that a purified or recombinant BMP needs a certain carrier to induce the *in vivo* cartilage or bone formation. This phenomenon was first explained as a result of rapid diffusion from the point of administration of BMP when it was applied to muscles or skin without a carrier. Thus, the BMP-carrier was considered to be a typical drug delivery system. But soon it was shown that the BMP-carrier is not merely a drug delivery system, but an important cell supporter for differentiation, since bone formation occurs only on the surface of the carrier (*14*).

In support of this concept, it was found that BMP-induced chondro- and osteogenesis are highly dependent upon the carrier used in the experimental system. The most widely

[1] This study was supported in part by Grants-in-Aid (Nos. 08557096, 07457437, 06557095, 05454495, and 04557078) from the Ministry of Education, Science, Sports and Culture of Japan.

[2] To whom correspondence should be addressed. Phone: +81-11-706-4231, FAX: +81-11-706-4877, E-mail: kuboki@den.hokudai.ac.jp

Abbreviations: ALP, alkaline phosphatase; BMP, bone morphogenetic protein.

used carrier of BMP is insoluble bone matrix, which is the decalcified and 4 M guanidine-extracted residues of bone powder or tips (*15*). Experiments with this carrier suggested that BMP is a cytokine which induces a process similar to endochondral ossification, that is, osteogenesis occurs only after chondrogenesis. However, by using fibrous collagen membrane as a carrier, Sasano *et al.* showed that BMP can induce direct bone formation, independent of cartilage formation (*6*).

Kuboki *et al.* showed that BMP induced only osteogenesis when porous particles of hydroxyapatite were used as a carrier, whereas only chondrogenesis occurred within a carrier of fibrous glass membrane (*14*). They concluded that vasculature is the crucial factor that determines osteogenesis or chondrogenesis. More recently, Saito *et al.* showed that BMP combined with a fibrous collagen membrane not only induces bone formation but also regenerates cementum and periodontal ligament when it is implanted into periodontal defects in the cat canine (*16*). These observations led us to the working hypothesis that BMP-induced cell differentiation is highly dependent on the cell substratum that is the matrix and on microenvironmental conditions, and that the cell substratum and the microenvironment are provided by the BMP-carrier.

The essential characteristics of BMP-carriers fall into three categories: (1) chemical, (2) physical, and (3) geometric. The first two categories are mainly concerned with biocompatibility, cell attachment, and affinity for biomolecules. These categories are well documented. However, the significance of the geometry of BMP-carriers has not been extensively studied and is not well understood.

Reddi and Huggins described the superior bone-inducing ability of coarse powder (420-850 μm) compared to fine powder (44-74 μm) of decalcified bone (*17*). Similarly, Sampath and Reddi reported the superiority of a coarse powders (74-420 μm) of demineralized bone matrix to fine powders (44-74 μm) (*18*). More recently, Repamonti and Reddi compared the bone-inducing ability of porous hydroxyapatite granules and disks with different pore sizes, 200 and 500 μm (*19*). They found that only the disks could induce bone formation, and that higher alkaline phosphatase activity was induced in disks of 500 μm pore size than in those of 200 μm pore size. However, the geometry of hydroxyapatite they used was replicated from the exoskeletal microstructure of corals of the genus *Prorites* for 200 μm and *Goniopora* for 500 μm, and thus there might have been a wide range of deviation in their average pore size, due to the biological origin of the materials. Also, the alkaline phosphatase activity that they measured did not necessarily reflect the amount of bone formation (*14*).

Thus, we decided to examine in detail the effect of pore size of the carrier on BMP function by using chemically synthesized and molded products of porous hydroxyapatite (*20*). We prepared five porous hydroxyapatites with pore sizes of 106-212, 212-300, 300-400, 400-500, and 500-600 μm, and which had the same porosity of 70% and the same form (blocks of approximately $5\times5\times1$ mm). BMP was combined with these porous hydroxyapatites, implanted subcutaneously into the back of rats, and the amounts of bone induced were compared.

MATERIALS AND METHODS

Preparation of Porous Hydroxyapatite Blocks—Hydroxyapatite powder was synthesized through two-stage hydrolysis of brushite ($CaHPO_4\cdot2H_2O$) according to the method of Monma and Kamiya (*21*). The first stage involves a structural change into apatite, and the second stage a compositional increase in the Ca/P ratio while retaining the apatite structure. The brushite powder was suspended and stirred in distilled water for 6 h. The temperature was maintained at 60°C, and the pH was adjusted to 8 with ammonium hydroxide solution. Solid products were filtered and washed with water, then suspended with calcium hydroxide in distilled water and stirred for 2 h. Temperature and pH were maintained at 70°C and 11, respectively. The products were filtered, washed and dried at 80°C.

Samples of the synthesized hydroxyapatite powders were heat-treated at 800°C for 2 h. The effect of heat treatment was estimated by X-ray diffractometry, infrared spectroscopy, specific surface area measurement and a solubility test. The specific surface area was determined to be 240 cm^2/g by measuring the adsorption of nitrogen gas. For the solubility test, 2.5 g of hydroxyapatite powder was suspended and stirred in 1,000 ml of physiological saline solution for 72 h, then filtered.

Synthesized hydroxyapatite powder was calcined at 800°C for 3 h and mixed with specific amounts of the acrylic beads of five diameters (Sekisui Plastics, Osaka): 106-212, 212-300, 300-400, 400-500, and 500-600 μm. The mixed powder was pressed in a disk-shaped mold of 20 mm in diameter and 4 mm in thickness. The mixing ratio was 70 vol%. The pellet was cold-isostatic pressed with a pressure of 300 MPa after vacuum-sealing in a natural rubber tube 0.1 mm thick. The compacted material was removed from the tubing and gradually heated in nitrogen gas up to 520°C to remove the polymer beads, then sintered in air at 1,200°C for 1 h.

One characteristic of the product was that its pores were interconnected, and spaces opened continuously into each particle (*20*).

Implantation of Carrier—Three disks of each pore size cut into blocks. Three sintered disks of each pore size were carefully sliced by use of a diamond disk cutter for the dental profession into blocks of $5\times5\times1$ mm (40 mg). The blocks were gently washed with a full volume of distilled water to remove any fine particles inside the pores that had been produced during the cutting. The blocks were sterilized at 150°C for 3 h. Then each block was mixed with 4 μg of recombinant human BMP-2 (a kind gift from Yamanouchi). The amount of the BMP-2 needed for reproducible ectopic osteogenesis in the system was determined previously by using porous particles of hydroxyapatite. Wistar strain male rats (about 60 g in weight) were anesthetized intraperitoneally with pentobarbital sodium (4 mg/100 g body weight). The back was shaved, cleaned with 70% alcohol and iodine, and cut by blunt dissection to form subcutaneous pockets. BMP-carrier composites were implanted carefully with tweezers in the subcutaneous pockets and sutured. The animals were killed with an overdose of ether at 1, 2, 3, or 4 wk after implantation. The implants and surrounding tissues which formed the clearly

discrete pellets were removed and subjected to biochemical analysis and histological observation.

Alkaline Phosphatase (ALP) Activity—Implanted pellets were lyophilized and stored frozen at −80°C until use. Samples were cut with scissors in a conical Eppendorf tube into fine powders of about 0.1 mm in particle size and mixed in 1 ml of 0.2% Nonidet P-40, 10 mM Tris-HCl, 1 mM $MgCl_2$, pH 7.5. ALP activity of the suspension was measured by the Kind-King phenylphosphate method (*22*).

Osteocalcin Content—Pulverized samples were decalcified with 40% formic acid at 4°C for 12 h, keeping the pH constant at 2.0 by addition of 40% formic acid. The decalcified solution was collected by centrifugation at 10,000×*g* for 30 min. The supernatant was dialyzed against distilled water and lyophilized. The samples were dissolved in phosphate buffer (0.123 M NaCl, 0.01 M NaH_2PO_4, 0.025 M $Na_4EDTA \cdot 2H_2O$, pH 7.4) for radioimmunoassay (RIA). Rat osteocalcin (Biomedical Technologies, USA) was used as a standard of osteocalcin. Goat anti-rat osteocalcin (Biomedical Technologies) was used as the first antibody. Donkey anti-goat IgG (Biomedical Technologies) was used as the second antibody. Rat osteocalcin was labeled with ^{125}I by the lactoperoxidase method (ICN Pharmaceuticals, USA). Four groups of plastic RIA tubes were prepared: nonspecific binding tubes (NSB), blank tubes, standard tubes containing 0.03-2.00 ng of osteocalcin/tube, and sample tubes. On the first day of the assay, 100 ml of the first antibody was added to each group except NSB. Tubes were incubated overnight at 4°C with gentle shaking. On the second day, 100 ml of approximately 2×10^5 cpm of ^{125}I-labeled rat osteocalcin was added to each tube, and the tubes were incubated overnight. On the third day, 1 ml of 2% second antibody was added to each tube, and the tubes were incubated for 2 h at 4°C, then centrifuged at 10,000×*g* for 30 min. The supernatant was carefully decanted, and the radioactivity of the pellets was counted in gamma counter for 2 min. The osteocalcin contents of samples were calculated from the standard curve.

RESULTS

Biochemical Analysis—Time-dependent changes of ALP activities and osteocalcin contents in the implanted ceram-

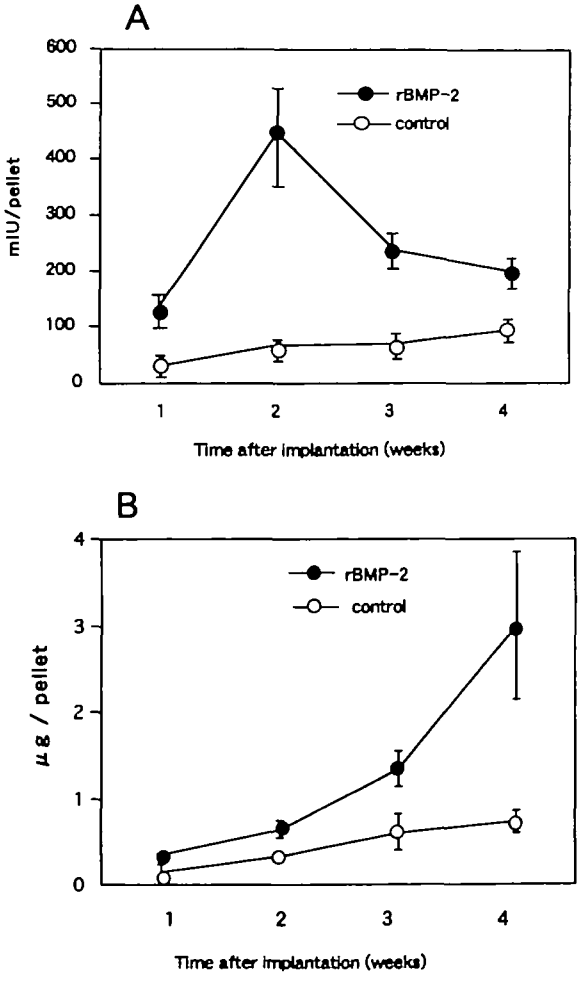

Fig. 1. **Time-dependent changes of alkaline phosphatase (ALP) activities (A) and osteocalcin contents (B) in the porous block of hydroxyapatite of pore size 106-212 μm with BMP (closed circles) and without BMP (open circles).** Vertical bars indicate standard deviation ($n=3$).

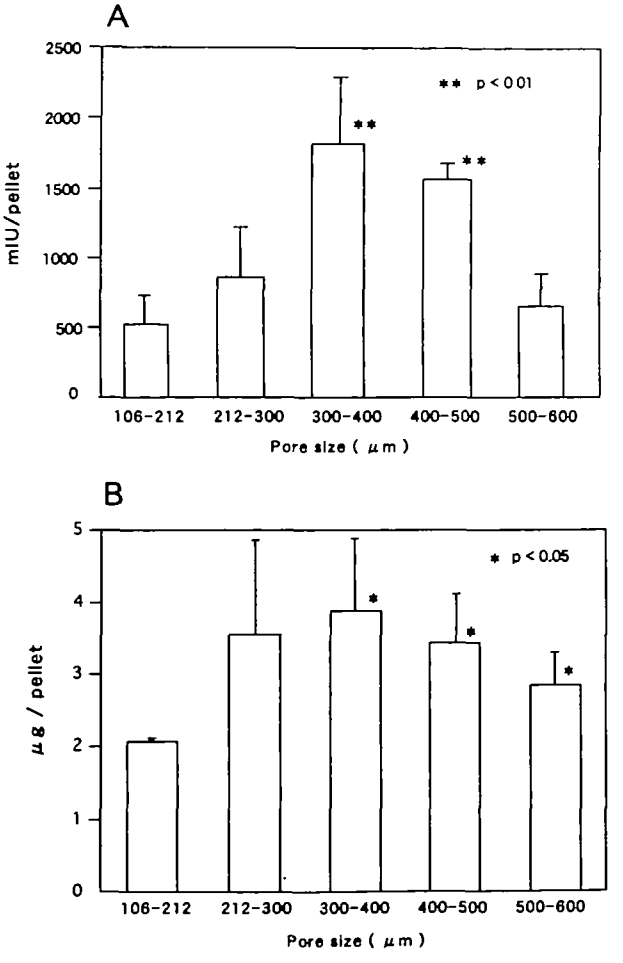

Fig. 2. **ALP activities (A) and osteocalcin contents (B) of implants of BMP mixed porous blocks of hydroxyapatite with different pore sizes.** Vertical bars indicate standard deviation ($n=3$). Values significantly different from that of the implant of pore size 106-212 μm are marked: $^*p<0.05$, $^{**}p<0.01$, by paired *t*-test analysis.

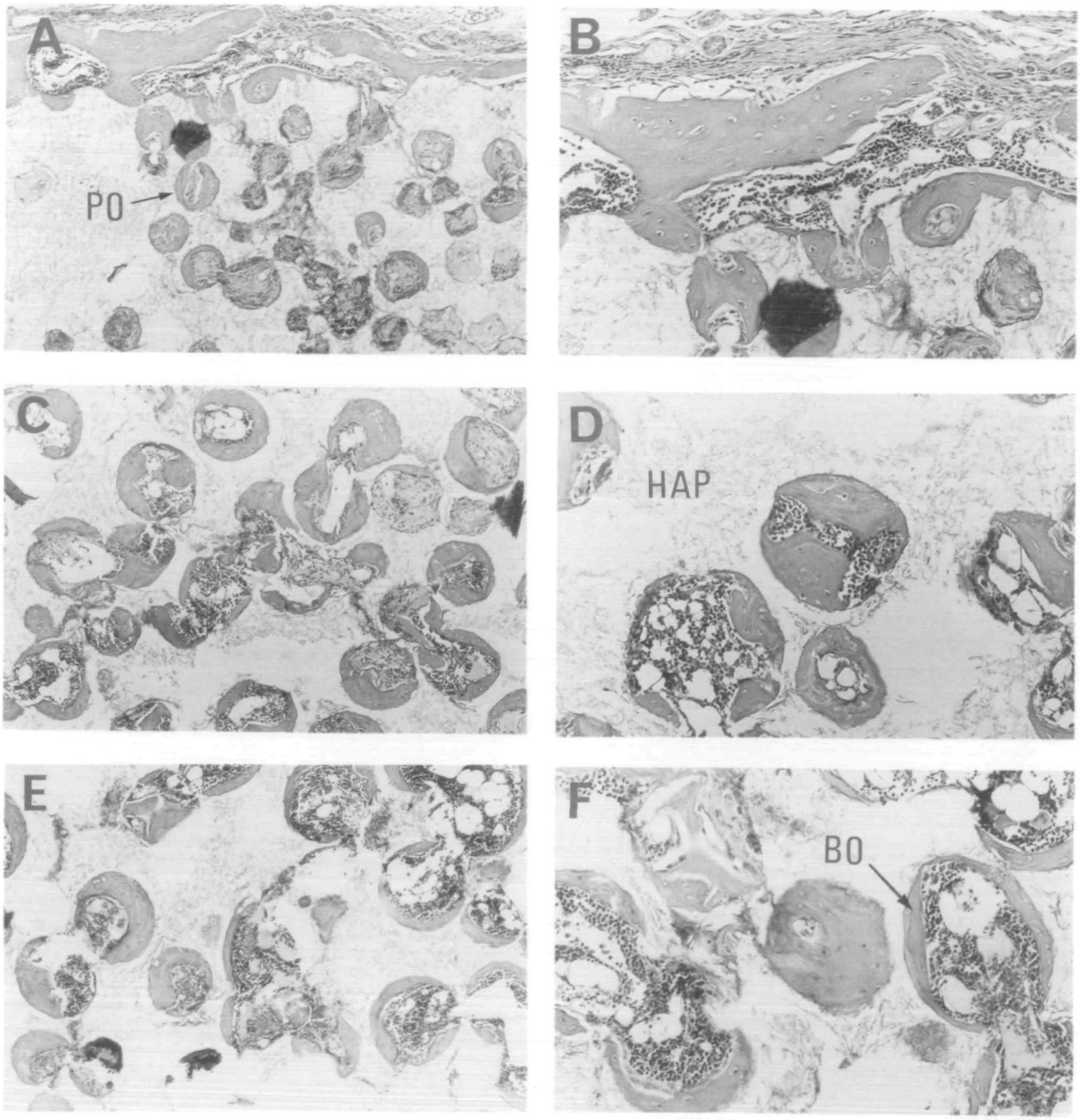

Fig. 3, A-F

ics with a pore-size range of 106-212 μm are shown in Fig. 1, A and B. The peak of alkaline phosphatase activities was detected at 2 wk after implantation, and the content of osteocalcin contents increased continuously for 4 wk, consistent with previous results in which insoluble bone matrix was used as a carrier (*7*). Thus, we decided to compare the implants with different pore sizes in terms of alkaline phosphatase activities at 2 wk (Fig. 2A) and osteocalcin contents at 4 wk after implantation (Fig. 2B).

The highest alkaline phosphatase activities and osteocalcin contents were both obtained with pore size of 300-400 μm. ALP activities with 300-400 μm pore implants were 3.5 times higher than with 106-212 μm pore implants, and 3.0 times higher than with 400-500 μm pore implants.

Osteocalcin contents with 300-400 μm pore implants were 2.0 times higher than with 106-212 μm pore implants. Osteocalcin contents of the implants with pore sizes larger than 300 μm were significantly higher than with those of 106-212 μm pore size.

Histological Observation—Histological observation together with biochemical analysis indicated that all the implanted BMP-carrier composites showed the osteogenic reaction. The high reproducibility of the bone-inducing reaction contrasted with that in previous reports (*11-13*), in which a certain percentage of implants failed to show the expected reaction.

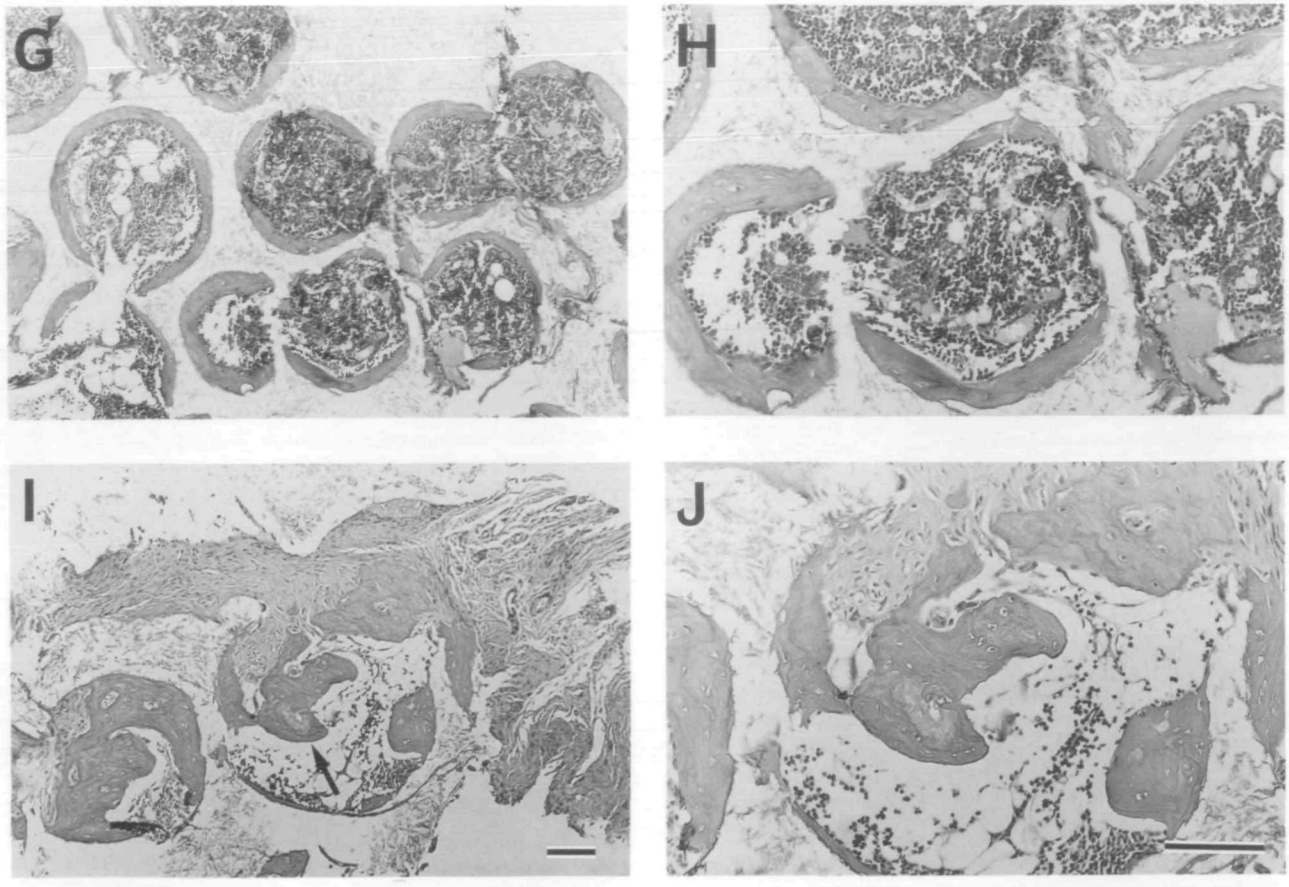

Fig. 3. **Microphotographs of cross-sections of BMP combined porous blocks of hydroxyapatite removed at 4 wk after implantation.** Pore sizes are: 106-212 μm in (A) and (B), 212-300 μm in (C) and (D), 300-400 μm in (E) and (F), 400-500 μm in (G) and (H), and 500-600 μm in (I) and (J). Original magnifications of photographs are $\times$75 for the left and $\times$150 for the right of each pair. A bar in the lower right corner of (I) and (J) indicates 100 μm. Pores are shown as multiple round structures in all photographs [indicated by PO in (A) for example]. Spaces other than pores [indicated by HAP in (D) for example] are occupied by hydroxyapatite. Bone formation [indicated by BO in (F) for example] was observed on the inner surface of almost all pores of up to 500 μm. In pores of 500-600 μm, bone was formed not only along the inner surface but also within the cavity of the pore [indicated by an arrow in (I)].

At 2 wk after implantation, the implants with different pore sizes showed similar histological changes. Pores were commonly filled with loose fibrous connective tissue at 1 wk, and the fibrous structure became more compact at 2 wk. At 3 wk, bone formation became histologically observed on the inner surface of the pores.

At 4 wk, we observed the histological characteristics of bone in the ceramics of all pore sizes. In the ceramics of 106-212 μm pore size, the bone structure on the surface of pores was accompanied by cement lines, indicated that bone remodeling occurred in this stage. Bone did not form in some pores. In the ceramics of 212-300 μm pore size, almost all pores were filled with bone. Interestingly, there was always a certain space for vascular tissue within a pore. We observed a similar feature in the porous particles of hydroxyapatite with average pore size of 150 μm (*23*). In the ceramics with pore sizes of 300-400 and 400-500 μm, bone tissues were accompanied by bone marrow cells and adipocytes within the pores. In some pores, capillaries and bone marrow cells were distinguishable side by side within the same space surrounded by bone. In the ceramics of 500-600 μm pore size, bone was formed not only along the inner surface of the pore but also within the pore cavity. Finally, a certain mechanical stability seemed to be required to maintain the bone lining of the inner wall of the pore. As shown in Fig. 3, as the pore size became larger than 300-400 μm, the lining of the inner wall became thinner. In the ceramics with pore size of 500-600 μm, the integrated formation of bone along the inner walls was no longer observed: bone occupied the cavity of the pores, but the rigid lining along the inner surface was interrupted (Fig. 3, [I] and [J]). In the 400-500 and 500-600 μm pores, multiple and larger capillaries appeared within a single pore, which was not observed in the pores of 300-400 μm and smaller. These observations suggested that the 300-400 μm pore size was most appropriate for Harvasian-type bone formation, leading to preferential formation of bone compared to the other pore sizes.

DISCUSSION

Hydroxyapatite as a Cell Substratum—To construct a connective tissue such as bone *in vivo*, we need not only techniques of molecular biology but also new concepts. We proposed that at least four factors need to be combined: cells, matrix, body fluid, and regulators (*1*). Above all, a

matrix as a three-dimensional cell substratum is crucially important to construct a tissue-like structure either *in vivo* or *in vitro*. Various forms of hydroxyapatite have been proved to be compatible cell substrata for osteogenic cells (*23-28*). For local orthotopic bone reconstruction, a porous form of hydroxyapatite has generally been considered to be more suitable for implantation than non-porous particles or solids. However, there is no definitive evidence concerning the optimal pore size for bone formation. This paper demonstrates for the first time that, under certain circumstances, a pore size of 300-400 μm was most effective for bone formation.

History of Geometric Effect—The effect of the geometry of the cell-substratum upon cell differentiation and growth was first described by Reddi and Huggins (*29*). They implanted two distinct particle sizes of decalcified bone powders containing BMP into rat skin, and found that the coarse powder with particle sizes of 420-850 μm induced more bone formation than the fine powder sized 44-74 μm. They also reported that when they implanted allogenic demineralized root of incisor, in which the apical end was closed, subcutaneously into rats, only cartilage was induced; but when they implanted the demineralized cylindroids of dentin, in which the both ends were open, bone was induced inside. Later, Sampath and Reddi (1984) showed more clearly that coarse powder (74-420 μm) induced bone formation, but fine powder (44-74 μm) did not (*18*). They emphasized the crucial importance of the geometry of the matrix in triggering the biochemical cascade of bone differentiation *in vivo*, but they did not touch upon the underlying mechanism. Shimazaki *et al.* (1985) reported that hydroxyapatite with pore size of 200-600 μm had superior osteogenic ability to that of 190-230 μm in the diaphyses of rabbit tibiae (*30*). Eggli *et al.* (1988) reported, on the contrary, that hydroxyapatite with pore size of 50-100 μm was superior to that of 200-400 μm (*31*). Recently, Ripamonti and Reddi (1992) compared the bone-inducing abilities of porous hydroxyapatite granules and disks with different porosities, 200 and 500 μm, as BMP carriers (*19*). They concluded that hydroxyapatite disks could induce bone formation but granular hydroxyapatite would not. Bone was induced in a higher amount in discs of 500 μm porosity than in those of 200 μm porosity. In contrast, Simmon and Ripamonti (1994) reported that porous particles of hydroxyapatite with sizes of 420-600 μm induced bone formation, while the block type did not (*32*). Thus, the effect of pore size on bone formation still seems to need extensive investigation.

Significance of the Present Study—We have already reported that two geometrically different solid-state carriers induce bone and cartilage in quite different manners when they are combined with BMP and implanted subcutaneously into rat (*14*). Porous hydroxyapatite with an average pore size of 150 μm induces direct bone formation on the inner surface of the pore, while a fibrous glass membrane with a fiber diameter of 1 μm induces cartilage formation in the inner area of the membrane. These results clearly demonstrated carrier-dependent phenotype expression in BMP-induced differentiation and further confirmed that BMP is able to induce not only cartilage formation but direct bone formation, which may be dependent upon the geometry of the carrier (*6*). It was explained that porous hydroxyapatite provided sufficient space for vasculature, while the tight network of the fibrous glass membrane allowed immature cells to penetrate into the membrane, but was too restricted for vascular formation.

The two carriers in our previous study (*14*) were different in geometry, but they were also composed of different materials, glass and hydroxyapatite. A more definite conclusion on the geometrical effect requires experiments using carriers that are geometrically different but composed of the same material. Thus, in the present study, we synthesized hydroxyapatite by the same method as before and prepared blocks of porous hydroxyapatite that differed only in pore size.

In Fig. 2, the osteocalcin contents in the 300-400 μm pores are the highest, clearly indicating this ceramic, combined with BMP, was most suitable for production of bone. Why this pore-size range worked more effectively than others for osteogenesis is explained in the following section in terms of vascularization, cell density, and mechanical stability for maintaining inner wall construction.

Why a Certain Pore Size Led to Maximal Bone Formation—The structure of a carrier that leads vascularization into the bulk of the carrier itself may be the most important geometrical factor for BMP-induced ectopic osteogenesis. This conclusion was deduced from the observation that a carrier which permits capillaries to penetrate its interior induces bone formation, while one which prevents such penetration, such as fibrous glass membrane with a mesh size of less than 1 μm, induces cartilage formation inside the carrier, but not bone formation (*14*). Also, non-porous hydroxyapatite in the form of solid spheres with a diameter of 300-500 μm induced neither bone nor cartilage formation (Kuboki *et al.*, in preparation). In the carrier used in this study, the interconnectedness of pores in the porous particles of hydroxyapatite might easily induce vasculature into the carrier. Pores must be larger than the diameter of active capillaries which can supply enough blood for bone formation, and this diameter was estimated to be approximately 50 μm from Fig. 3. Development of a single capillary should allow formation of an osteon-like structure.

Detailed observation of secondary osteon formation in Harversian type of bone tissue shows that osteons measure from 200 to 300 μm in diameter, the diameter of the central canal varies from 20 to 50 μm and the wall thickness measures up to 80 μm (*33*). We hypothesized that the ready-made structure of a pore of 300-400 μm in diameter favors the formation of osteon-like structures. Generally, the inner walls of the concave tubing structure of interconnecting pores will provide the physical environment required to generate a high cell density than a convex or flat surface. Thus, it is considered that the concave surface provided by the pores of the ceramics of 300-400 μm in diameter will be ideal for generating a cell density adequate for osteogenesis.

Finally, a certain mechanical stability seemed to be required for maintaining the inner wall of the pore in which bone was constructed. As shown in Fig. 3, as the pore size became larger than 300-400 μm, the inner wall became thinner, and in the ceramics with pores of 500-600 μm, integrated formation of bone no longer occurred along the inner walls (Fig. 3(I) and (J)). Bone formed in the 500-600 μm pores occupied the cavities of the pores, and the rigid lining along the inner surface was interrupted (Fig. 3, (I)

and (J)). In the 400-500 μm and 500-600 μm pores, multiple and larger capillaries appeared within a single pore, which were not observed in the pores of 300-400 μm or smaller. These observations suggested that the 300-400 μm pore size was most appropriate for Harvasian osteoid formation, thereby leading to a preferential formation of bone compared to the other pore sizes.

Usefulness and Conclusion—The potential usefulness of these findings for both experimental and clinical tissue construction is enormous. For most anchorage-dependent cells to achieve differentiation, probably with an exception of chondrocytes, vasculature is obviously one of the crucial factors. A major problem in creating tissues artificially *in vivo* and *in vitro* is how to provide vasculature for cells, since a mere mass of cells easily results in necrosis. Our finding concerning the pore size in the BMP-induced differentiation system will provide a model applicable for constructing other devices for cell substrata, although the optimal size for pores of the substrata will vary from one type of cell to another. Replacing the hydroxyapatite used in this study with a bio-resorbable material such as tricalcium phosphate or polylactic acid will open a new avenue for tissue engineering.

Our proposition of four factors for bone formation, described in the beginning of this paper, indicates that a proper *in vivo* supply of matrices and regulators (BMP) is sufficient for successful ectopic bone formation. Thus, we focused on the geometry of the cell substratum and determined the optimal pore size for bone formation to be 300-400 μm. We also found that this matrix factor is closely related with the supply of body fluid, that is, vasculature. Our discovery seems to reveal a new paradigm of biology, an artificial matrix to create tissues and perhaps even organs of the animal body.

REFERENCES

1. Kuboki, Y., Yamaguchi, H., Yokoyama, A., Murata, M., Takita, H., Tazaki, M., Mizuno, M., Hasegawa, T., Iida, S., Shigenobu, K., Fujisawa, R., Kawamura, M., Atuta, T., Matumoto, A., Kato, H., Zhou, H.-Y., Ono, I., Takeshita, N., and Nagai, N. (1991) *The Bone-Biomaterials Interface. Osteogenesis Induced by BMP-Coated Biomaterials: Biochemical Principles of Bone Reconstruction in Dentistry*, pp. 127-138, Univ. Tront Press, Tronto
2. Mizuno, M. and Kuboki, Y. (1995) TGF-beta accelerated the osteogenetic differentiation of bone marrow cells induced by collagen matrix. *Biochem. Biophys. Res. Commun.* **211**, 1091-1098
3. Fujisawa, R. and Kuboki, Y. (1995) Further characterization of interaction between bone sialoprotein (BSP) and collagen. *Calcif. Tissue. Int.* **56**, 140-144
4. Takita, H. and Kuboki, Y. (1995) Conformational changes of bovine bone osteonectin induced by interaction with calcium. *Calcif. Tissue. Int.* **56**, 559-565
5. Shigenobu, K., Kaneda, K., Nagai, N., and Kuboki, Y. (1993) Localization of bone morphogenetic protein-induced bone and cartilage formation on a new carrier. *Ann. Chir. Gynaecol.* **82**, 85-90
6. Sasano, Y., Ohtani, E., Narita, K., Kagayama, A., Murata, M., Saito, T., Shigenobu, K., Takita, H., Mizuno, M., and Kuboki, Y. (1993) BMPs induce direct bone formation in ectopic sites independent of the endochondral ossification in vivo. *Anat. Rec.* **236**, 373-380
7. Kobayashi, D., Takita, H., Mizuno, M., Totsuka, Y., and Kuboki, Y. (1996) Time-dependent expression of bone sialoprotein fragments in osteogenesis induced by bone morphogenetic protein. *J. Biochem.* **119**, 475-481
8. Urist, M.R. (1965) Formation by autoinduction. *Science* **150**, 893-899
9. Wozney, J.M., Rosen, V., Celeste, A.J., Mitsock, L.M., Whitters, M.J., Kriz, R.W., Hiwick, R.M., and Wang, E.A. (1988) Novel regulators of bone formation. *Science* **242**, 1528-1534
10. Inada, M., Katagiri, T., Akiyama, S., Namiki, M., Komaki, M., Yamaguchi, A., Kamoi, K., Rosen, V., and Suda, T. (1996) Bone morphogenetic protein-12 and 13 inhibit terminal differentiation of myoblast, but do not induce their differentiation into osteoblasts. *Biochem. Biophys. Res. Commun.* **222**, 317-322
11. Wang, E.A., Rosen, V., D'Alessandro, J.S., Bauduy, M., Cordes, P., Harada, T., Isreal, D.I., Hewick, R.M., Kerns, K.M., Lapan, P., Luxenberg, D.P., McQuaid, D., Moutsatsos, I.K., Nove, J., and Wozney, J.M. (1990) Recombinant human bone morphogenetic protein induces bone formation. *Proc. Natl. Acad. Sci. USA* **97**, 2220-2224
12. Hammonds, R.G., Jr., Schwall, R., Dudley, A., Berkemeier, L., Lai, C., Lee, J., Cunningham, N., Reddi, A.H., Wood, W.I., and Mason, A.J. (1991) Bone-inducing activity of mature BMP-2b produced from a hybrid BMP-2a/2b precursor. *Mol. Endocrinol.* **5**, 149-155
13. Sampath, T.K., Maliakal, J.C., Hauschka, P.V., Jones, W.K., Sasak, H., Tucker, R.F., White, K.H., Coughlin, J.E., Tucker, M.M., Pang, R.H.L., Corbett, C., Oskaynak, E., Oppermann, H., and Rueger, D.C. (1992) Recombinant human morphogenetic protein-1 (hOP-1) induces new bone formation *in vivo* with a specific activity comparable with natural bovine osteogenic protein and stimulates osteoblast proliferation and differentiation *in vitro*. *J. Biol. Chem.* **27**, 20352-20362
14. Kuboki, Y., Saito, T., Murata, M., Takita, H., Mizuno, M., Inoue, M., Nagai, N., and Pool, R. (1995) Two distinctive BMP-carriers induce zonal chondrogenesis and membranous ossification,respectively; geometrical factors of matrices for cell-differentiation. *Connect. Tissue. Res.* **32**, 219-226
15. Sampath, T.K. and Reddi, A.H. (1981) Dissociative extraction and reconstruction of extracellular matrix components involved in local bone differentiation. *Proc. Natl. Acad. Sci. USA* **78**, 7599-7603
16. Saito, A., Kato, H., and Kuboki, Y. (1994) A study of periodontal regererative therapy using BMP in horizontal bone defects. *Jpn. J. Periodont.* **36**, 810-822
17. Reddi, A.H. and Huggins, C.B. (1973) Influence of geometry of transplanted tooth and bone on transformation of fibroblasts. *Proc. Soc. Exp. Biol. Med.* **143**, 634-637
18. Sampath, T.K. and Reddi, A.H. (1984) Importance of geometry of extracellular matrix in endochondral bone differentiation. *J. Cell. Biol.* **98**, 2192-2197
19. Ripamonti, U., Ma, S., and Reddi, A.H. (1992) The critical role of geometry of porous hydroxyapatite delivery system in induction of bone by osteogenin, a bone morphogenetic protein. *Matrix* **12**, 202-212
20. Itoh, H., Wakisaka, Y., Ohnuma, Y., and Kuboki, Y. (1994) A new porous hydroxyapatite ceramics prepared by cold isostatic pressing and sintering synthesized flaky powder. *Dental Mater. J.* **13**, 25-35
21. Monma, H. and Kamiya, T. (1987) Preparation of hydroxyapatite by the hydrolysis of brushite. *J. Mater. Sci.* **22**, 4247-4250
22. Kind, P.R.N. and King, E.J. (1954) Estimation of plasma phosphate by determination of hydrolizes phenol with amino-antipyrine. *J. Clin. Pathol.* **7**, 322-326
23. Ozawa, S. and Kasugai, S. (1996) Evaluation of implant materials (hydroxyapatite, glass-ceramics, titanium) in rat bone marrow stromal cell culture. *Biomaterials* **17**, 23-29
24. Hench, L.L. and Wilson, J. (1984) Surface-active biomaterials. *Science* **226**, 630-636
25. Jarcho, M. (1981) Calcium phosphate ceramics as hard tissue prosthetics. *Clin. Orthop.* **157**, 259-278
26. Meffert, R.M., Thomas, J.R., Hamilton, K.M., and Brownstein, C.N. (1985) Hydroxyapatite as an alloplastic graft in the treatment of human periodontal osseous defects. *J. Periodontol.* **56**, 63-73

27. Ono, I., Ohura, T., Murata, M., Yamaguchi, H., Ohnuma, Y., and Kuboki, Y. (1992) A study on bone induction in hydroxyapatite combined with bone morphogenetic protein. *Plast. Reconstr. Surg.* **90**, 870-879
28. Ono, I., Gunji, H., Suda, K., Kaneko, F., Murata, M., Saito, T., and Kuboki, Y. (1995) Bone induction of hydroxyapatite combined with bone morphogenetic protein and covered with periosteum. *Plast. Reconstr. Surg.* **95**, 1265-1272
29. Reddi, A.H. and Huggins, C.B. (1973) Influence of geometry of transplanted tooth and bone on transformation of fibroblast. *Proc. Soc. Exp. Biol. Med.* **143**, 4634-4637
30. Shimazaki, K. and Mooney, V. (1985) Comparative study of porous hydroxyapatite and tricalcium phosphate as bone substitute. *J. Orthop. Res.* **3**, 301-310
31. Eggli, P.S., Muller, W., and Schneck, R.K. (1988) Porous hydroxyapatite and tricalcium phosphate cylinders with two different pore size range implanted in the cancellous bone of rabbit. *Clin. Orthop.* **232**, 127-138
32. Simmon, P.E. and Ripamonti, U. (1994) Bone differentiation in porous hydroxyapatite in baboons is regurated by the geometry of the substratum: implantations for reconstructive craniofacial surgery. *Plast. Reconstr. Surg.* **93**, 959-966
33. Jaworski, Z.F.G. (1992) Haversian systems and haversian bone in *Bone* (Brian, K.H., ed.) Vol. 4, pp. 21-45, CRC Press, London